Regge Cuts from Off-Mass-Shell and On-Mass-Shell Nonplanar Feynman-Like Duality Diagrams*

R. J. Rivers and J. J. G. Scanio
The Enrico Fermi Institute, The University of Chicago, Chicago, Illinois 60637
(Received 14 August 1969)

In a theory of Feynman-like diagrams compatible with duality, we compare the Regge cut given by the simplest nonplanar diagrams (the unrenormalized two-Reggeon cut) with the Regge cut obtained from the same diagrams in the double-scattering formalism in which the intermediate two-body state is put on one or several of its mass shells. The cut spectral functions are shown to be simply related at the branch point, but the different ways of incorporating the signature factors in the two methods give rise to zeros in the leading cut amplitudes at different places. The predictions of a double-scattering Regge cut are thus likely to be qualitatively similar but quantitatively different from those of the Feynman-like Regge cut.

1. INTRODUCTION

In addition to poles in the angular momentum plane, the unitarity equations for the high-energy two-body scattering amplitudes strongly suggest[1] that cuts are also present.

Moreover, there are now data on a large variety of high-energy two-body scattering processes that show that Regge poles by themselves are unable to explain more than the crude features of forward and near-forward high-energy two-body scattering.[2]

Phenomenological models for Regge cuts that introduce few parameters in addition to the Regge-pole parameters are thus becoming more important. Many authors[3] have taken multiple scattering in a single channel (e.g., the initial- and final-state interactions of the usual absorption model for charge-exchange scattering) as a model for Regge cuts. Except for roughly determined scale factors,[2] no new parameters beyond those used to describe the Regge poles are needed. Such cuts have been shown[2,4] to have the correct features to explain the discrepancies between the predictions of a theory with Regge poles alone and the experimental data.

There are two difficulties with such a relativistic phenomenological theory in which the intermediate two-body states in the multiple scattering are on their mass shells.

First, it is not obvious how the off-mass-shell intermediate-state contribution to the multiple scattering is supposed to be canceled. Moreover, it has been shown for certain diagrams in relativistic field theory[5] that the off-mass-shell intermediate-state contribution asymptotically dominates the on-mass-shell contribution.

Second, because multiple scattering can be considered as a unitarization of the Regge-pole amplitude in one channel only, it is difficult to incorporate crossing symmetry in a nonarbitrary manner. Because of the connection between crossing and signature, this can lead to incrorrect signature in the asymptotic cut amplitudes. This requires the addition of counterterms of dubious physical significance to restore the correct signature factors.

Because of these difficulties, it is interesting to compare the Regge cuts due to off-mass-shell and on-mass-shell intermediate states in a relativistic theory that explicitly contains Reggeization, crossing symmetry, and a phenomenologically plausible particle mass spectrum (e.g., indefinitely rising Regge trajectories).

Recently a theory of Feynman-like diagrams has been proposed[6–8] in which the generalized Veneziano amplitude[9] plays the role of a Born term. This theory explicitly incorporates duality (with the mass spectrum of the Veneziano representation), crossing symmetry, and Reggeization.

The Feyman-like diagrams can be classified as planar or nonplanar. The planar Feynman-like diagrams provide renormalization corrections[6] to the basic Born term, giving a right-hand cut to the Regge trajectories. The nonplanar diagrams in general give rise to Regge cuts.[7,8]

The simplest nonplanar diagram of Fig. 1(a) (giving rise to a Regge cut due to the exchange of two Regge poles) has been studied in detail in Ref. 7. This diagram stands in the same relation to the subset of nonplanar diagrams that give the renormalized Regge cut (due to the exchange of two Regge poles) as the Veneziano Born

* Supported in part by the U. S. Atomic Energy Commission.

[1] S. Mandelstam, Nuovo Cimento **30**, 1127 (1963); **30**, 1148 (1963); V. N. Gribov, I. Ya. Pomeranchuk, and K. T. Ter-Martirosyan, Yadern. Fiz. **2**, 361 (1965) [English transl.: Sov. J. Nucl. Phys. **2**, 258 (1966)].

[2] F. Henyey, G. L. Kane, J. Pumplin, and M. Ross, Phys. Rev. Letters **21**, 946 (1968); Phys. Rev. **182**, 1579 (1969); F. Henyey, K. Kajantie, and G. L. Kane, Phys. Rev. Letters **21**, 1782 (1968); R. J. Rivers, Nuovo Cimento **63A**, 697 (1969).

[3] R. C. Arnold, Phys. Rev. **140**, B1022 (1965); L. Van Hove, Phys. Letters **24B**, 183 (1967); E. J. Squires, *ibid.* **26B**, 461 (1968); **26B**, 736(E) (1968); J. Finkelstein and M. Jacob, Nuovo Cimento **56A**, 681 (1968).

[4] See, for example, N. White, Phys. Letters **27**, 93 (1968); F. Schrempp, Nucl. Phys. **B6**, 487 (1968); R. J. Rivers and L. M. Saunders, Nuovo Cimento **58A**, 385 (1968); C. Michael, Nucl. Phys. **B8**, 431 (1968); R. C. Arnold and M. L. Blackmon, Phys. Rev. **176**, 2083 (1968).

[5] M. E. Ebel and R. J. Moore, Phys. Rev. **177**, 2470 (1969).

[6] K. Kikkawa, B. Sakita, and M. A. Virasoro, Phys. Rev. **184**, 1701 (1969); K. Bardakci, M. B. Halpern, and J. A. Shapiro, *ibid.* **185**, 1910 (1969).

[7] K. Kikkawa, Phys. Rev. **185**, 2249 (1969).

[8] K. Kikkawa, S. Klein, B. Sakita, and M. A. Virasoro, (to be published).

[9] G. Veneziano, Nuovo Cimento **58A**, 190 (1968).

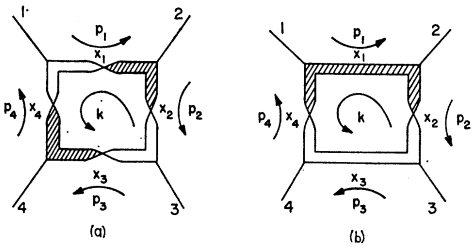

FIG. 1. Essentially nonplanar diagrams.

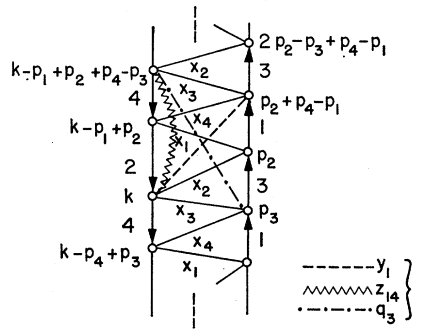

FIG. 2. Dual diagram associated with Fig. 1(a). Most of the dependent lines are omitted. It can have infinite extension.

term stands to the renormalized Regge pole amplitude due to the sum of all planar diagrams. It is likely that the moving cut given by Fig. 1(a) has many features of the renormalized two-Reggeon exchange cut.

In this paper we shall compare the Regge cut given by Fig. 1 (treated as Feynman-like diagrams in scalar particle scattering) with the Regge cut obtained from Fig. 1 by putting the two-particle intermediate state on the mass shell of the external scalar particles.

Although neither of the Regge poles exchanged in Fig. 1 is the Pomeranchukon (which is probably an infinite iteration of a nonplanar diagram), Fig. 1 has phenomenological interest in that it has been suggested[10] that double-charge-exchange scattering (e.g., $K^-p\to\pi^+\Sigma^-$) proceeds by repeated single-charge-exchange scattering.

In Sec. 2 we shall evaluate the leading-cut contribution of Fig. 1 in considerable detail. In Sec. 3 we evaluate the double-scattering cut from the zero-spin mass-shell intermediate state in Fig. 1. We conclude with a brief discussion of the double-scattering cuts due to higher-spin intermediate states.

2. CUT FROM NONPLANAR DIAGRAMS

We take the generalized Veneziano amplitude for the scattering of scalar particles to be

$$V(s,t)=\int_0^1 dx\, x^{-\alpha(s)-1}(1-x)^{-\alpha(t)-1}f(x)\,, \quad (2.1)$$

where, for simplicity, $\alpha(s)=\alpha(0)+s$ and $f(x)\equiv f(1-x)$ to preserve $s\leftrightarrow t$ crossing. The amplitude $V(s,t)$ has poles in the s and t channels.

The amplitude describing Fig. 1(a) has been essentially given in Ref. 7. We repeat the calculation here in more detail.

In Fig. 2 we give the dual diagram of Fig. 1(a). The independent variables x_i $(i=1,2,3,4)$ correspond to the sides of the box in Fig. 1(a). The dependent variables (corresponding to different triangulations of the dual diagram) can be obtained in terms of the x_i by the methods of Ref. 6 and 7 (reproduced in the Appendix). We classify the dependent variables by the number of lines x_i that they cross in the following way:

(i) The line y_i crosses x_i once, and x_j $(i\neq j)$ not at all.
(ii) The line z_{ij} crosses x_i x_j once, and x_k $(k\neq i,\ j)$ not at all.
(iii) The line q_i crosses x_k $(k\neq i)$ once, and x_i not at all.

All other dependent variables (i.e., lines which cross all the x_i at least once) are ignored, to be justified *a posteriori*.

The amplitude describing Fig. 1(a) is given by[7,11]

$$I^{(a)}(s,t)=\int d^4k\prod_i dx_i\prod_i x_i^{-\alpha[(p_i-k)^2]-1}\times\prod_i y_i^{-\alpha[(p_{i+1}-p_i+p_{i-1}-k)^2]-1}\times\prod_i q_i^{-\alpha[(-p_{i-1}+2p_i-p_{i+1}+p_{i+2}-k)^2]-1}\times(z_{12}z_{23}z_{34}z_{41})^{-\alpha(u)-1}R(x_1,x_2,x_3,x_4)\,, \quad (2.2)$$

where R is an almost arbitrary singularity-free spectral function invariant under $x_1\leftrightarrow x_3$, $x_2\leftrightarrow x_4$, and $x_i\to x_{i+1}$. If the mass of the external particles is m, we have $s+t+u=4m^2$, where $s=(p_2-p_4)^2$ and $t=(p_1-p_3)^2$. For simplicity, we have taken the same parent trajectory α everywhere, with $\alpha(m^2)=0$.

Performing the d^4k integration, we have

$$I^{(a)}(s,t)=-i\pi^2\int\frac{\prod_i dx_i}{\ln^2\prod_i x_iy_iq_i}\left(\prod_i x_iy_iq_i\right)^{-\alpha(0)-1}\times(z_{12}z_{23}z_{34}z_{41})^{-\alpha(0)-1}R(x_1,x_2,x_3,x_4)\times\exp[-(fs+gt+hm^2)]\,, \quad (2.3)$$

[10] R. J. Rivers, Nuovo Cimento **57A**, 174 (1968); C. B. Chiu and J. Finkelstein, *ibid.* **59A**, 92 (1969); C. Michael, talk presented at the Conference on Regge Cuts, Madison, Wisc. (unpublished).

[11] In Ref. 7, two of the z's and the q_i's were omitted. Such an omission affects the quantitative results only slightly.

where

$$f\ln\prod_i(x_iy_iq_i)=-\ln\prod_i(x_iy_iq_i)\ln(z_{12}z_{23}z_{34}z_{41})+\ln(x_2/y_2)\ln(x_4/y_4)+\ln q_2\ln q_4$$
$$-6\ln(q_2q_4)\ln(q_1q_3)-\ln(y_1y_3)\ln(x_1x_3y_2^2y_4^2)-\ln(q_1q_3)\ln(x_1x_3x_2^2x_4^2y_1^4y_3^4)$$
$$-\ln(q_2q_4)\ln(x_1^2x_3^2y_2^3y_4^3)-\ln q_2\ln(x_2y_4)-\ln q_4\ln(x_4y_2)\,, \quad (2.4)$$

$$g\ln\prod_i(x_iy_iq_i)=-\ln\prod_i(x_iy_iq_i)\ln(z_{12}z_{23}z_{34}z_{41})+\ln(x_1/y_1)\ln(x_3/y_3)+\ln q_1\ln q_3$$
$$-6\ln(q_2q_4)\ln(q_1q_3)-\ln(y_2y_4)\ln(x_2x_4y_1^2y_3^2)-\ln(q_2q_4)\ln(x_2x_4x_1^2x_3^2y_2^4y_4^4)$$
$$-\ln(q_1q_3)\ln(x_2^2x_4^2y_1^3y_3^3)-\ln q_1\ln(x_1y_3)-\ln q_3\ln(x_3y_1)\,, \quad (2.5)$$

$$h\ln\prod_i(x_iy_iq_i)=4\ln\prod_i(x_iy_iq_i)\ln(z_{12}z_{23}z_{34}z_{41})+\ln(x_1x_3)\ln(x_2x_4)+\ln(x_1x_3)\ln(y_2y_4y_1^4y_3^4)$$
$$+\ln(x_2x_4)\ln(y_1y_3y_2^4y_4^4)+9\ln y_1y_3\ln y_2y_4+\ln(x_1x_3)\ln(q_1^4q_3^4q_2^9q_4^9)+\ln(x_2x_4)\ln(q_2^4q_4^4q_1^9q_3^9)$$
$$+\ln(y_1y_3)\ln(q_1^{16}q_3^{16}q_2q_4)+\ln(y_2y_4)\ln(q_2^{16}q_4^{16}q_1q_3)+25\ln(q_1q_3)\ln(q_2q_4)\,. \quad (2.6)$$

As shown in Ref. 7, the leading asymptotic behavior of $I(s,t)$ as $s\to\infty$ is given by the region of integration $x_1=x_3=0$, $x_2=x_4=\frac{1}{2}$. We thus only have to include those dependent variables that cross either x_1 or x_3 once. This provides the *a posteriori* justification for our neglect of variables other than y, z, and q in Eq. (2.2). Using the parametrization of Ref. 7,

$$x_1=\rho\lambda\,,\quad x_3=\rho(1-\lambda)\,,$$
$$\ln(x_2/y_2)=\xi(-2\rho\ln\rho)^{1/2}\,, \quad (2.7)$$
$$\ln(x_4/y_4)=\eta(-2\rho\ln\rho)^{1/2}\,,$$

we calculate the leading behavior of $I^{(a)}(s,t)$ as $s\to\infty$ to be

$$I^{(a)}(s,t)=\tfrac{1}{8}i\pi^2\int\frac{d\rho d\lambda d\xi d\eta}{\ln^2[\frac{1}{16}\rho^2\lambda(1-\lambda)]}\rho^2\ln\rho$$
$$\times[\tfrac{1}{16}\rho^2\lambda(1-\lambda)]^{-\alpha(0)-1}R(0,\tfrac{1}{2},0,\tfrac{1}{2})4^{2m^2}$$
$$\times\{4\rho[\lambda(1-\lambda)]^{1/2}\}^{-t/2}\exp[-\rho s(1-\xi\eta)]\,. \quad (2.8)$$

The Mellin transform of $I^a(s,t)$ is thus given as

$$\tilde I^{(a)}(l,t)=\tfrac{1}{2}i\pi^2R(0,\tfrac{1}{2},0,\tfrac{1}{2})2^{-t}\Gamma(-l)$$
$$\times\int_{-\infty}^{\infty}d\xi d\eta[1-\xi\eta+i\tilde\epsilon]^l$$
$$\times\int_0^1 d\lambda[\lambda(1-\lambda)]^{-1/2[2\alpha(t/4)+2]}$$
$$\times\int_0^{\rho(\lambda)}d\rho\frac{\rho^{l-2\alpha(t/4)}\ln\rho}{\ln^2\{\rho[\frac{1}{16}\lambda(1-\lambda)]^{1/2}\}}\,, \quad (2.9)$$

where

$$\tilde\epsilon=\epsilon(1-\xi\eta)/|1-\xi\eta|\,,\quad \epsilon>0\,,\ s>0\,,$$

and the upper bound of the ρ integration $\rho(\lambda)$ is given by

$$\rho(\lambda)=(1-\lambda)^{-1}\,,\quad 0\le\lambda\le\tfrac{1}{2}$$
$$=\lambda^{-1}\,,\quad \tfrac{1}{2}\le\lambda\le1\,. \quad (2.10)$$

Performing the ξ, η integrations in Eq. (2.9), $\tilde I^{(a)}(l,t)$ can be written as

$$\tilde I^{(a)}(l,t)=-\pi^3R(0,\tfrac{1}{2},0,\tfrac{1}{2})2^{-t}\frac{\Gamma(-l)}{l+1}\int_0^{1/2}2d\lambda$$
$$\times\int_{-\infty}^{\alpha_c(t)}dj\frac{[\lambda(1-\lambda)]^{-1/2(j+1)-1}}{4^{\alpha_c(t)-j}}(1-\lambda)^{j-l}$$
$$\times\left[\frac{1}{l-j}+\frac{[\alpha_c(t)-l]}{(l-j)^2}X(\lambda)\right], \quad (2.11)$$

where

$$X(\lambda)=[\ln\tfrac{1}{16}\lambda(1-\lambda)]\{\ln[\lambda/16(1-\lambda)]\}^{-1}, \quad (2.12)$$

and $\alpha_c(t)$ is the two-Reggeon-cut branch point $\alpha_c(t)=2\alpha(\frac{1}{4}t)-1$.

Equation (2.11) shows the existence of a moving cut at $l=\alpha_c(t)$ and a fixed pole at $l=-1$.[12] It may be that an infinite iteration of the nonplanar diagram Fig. 1(a) converts this simple pole at $l=-1$ into an essential singularity.

In this paper, however, we are only concerned with the moving cut at $l=\alpha_c(t)$. Equation (2.11) gives rise to a cut amplitude

$$I_{\rm cut}{}^{(a)}(s,t)=\int_{-\infty}^{\alpha_c(t)}dj\,s^j\rho_{\rm cut}(j,t)\,, \quad (2.13)$$

where $\rho_{\rm cut}(j,t)$ is given by

$$\rho_{\rm cut}(j,t)=-\pi^3R(0,\tfrac{1}{2},0,\tfrac{1}{2})2^{-t}\Gamma(-j-1)4^{j-\alpha_c(t)}$$
$$\times\int_0^1 d\lambda[\lambda(1-\lambda)]^{-1/2(j+1)-1}$$
$$\times\{1+\tfrac{1}{2}[\alpha_c(t)-j]\ln\tfrac{1}{16}\lambda(1-\lambda)\}\,. \quad (2.14)$$

[12] V. N. Gribov and I. Ya. Pomeranchuk, Phys. Letters **2**, 232 (1962).

Asymptotically, Eq. (2.13) can be integrated by parts to give

$$I_{\rm cut}{}^{(a)}(s,t)\sim\frac{s^{\alpha_c(t)}}{\ln s}\rho_{\rm cut}(\alpha_c(t),t)[1+O(1/\ln s)]. \quad (2.15)$$

From Eq. (2.14) we see that $\rho_{\rm cut}(\alpha_c(t),t)$ is given by

$$\rho_{\rm cut}(\alpha_c(t),t)=-\pi^3R(0,\tfrac{1}{2},0,\tfrac{1}{2})2^{-t}\Gamma^2(-\alpha(\tfrac{1}{4}t)). \quad (2.16)$$

Let us now consider Fig. 1(b), the diagram obtained from Fig. 1(a) by $s\leftrightarrow u$ crossing. We immediately see from Eqs. (2.3) and (2.8) that this diagram gives a cut amplitude

$$I_{\rm cut}{}^{(b)}(s,t)=\int_{-\infty}^{\alpha_c(t)}dj\,e^{-i\pi j}s^j\rho_{\rm cut}(j,t) \quad (2.17)$$

for $s\to\infty$ above an arbitrarily narrow wedge containing the real axis.

The total cut amplitude

$$I_{\rm cut}(s,t)=I_{\rm cut}{}^{(a)}(s,t)+I_{\rm cut}{}^{(b)}(s,t)$$
$$=\int_{-\infty}^{\alpha_c(t)}dj\,s^j(1+e^{-i\pi j})\rho_{\rm cut}(j,t) \quad (2.18)$$

has the correct signature, and for $s\to\infty$ above the wedge

$$I_{\rm cut}(s,t)\sim(s^{\alpha_c(t)}/\ln s)(1+e^{-i\pi\alpha_c(t)})$$
$$\times\rho_{\rm cut}(\alpha_c(t),t)[1+O(1/\ln s)], \quad (2.19)$$

where $\rho_{\rm cut}(\alpha_c(t),t)$ is given in Eq. (2.16).

We compare this with the double-scattering-cut spectral function in Sec. 3.

3. ZERO-SPIN MASS-SHELL DOUBLE-SCATTERING CUT

The Regge cut due to double scattering in which the intermediate two-body state in Fig. 1(a) is put on the external-particle zero-spin mass shell can be obtained directly from Eq. (2.2).

Let us write Eq. (2.2) as

$$I^{(a)}(s,t)=\int d^4k\,I(k), \quad (3.1)$$

where $I(k)$ is written as

$$I(k)=\int\prod_i dx_iI(k;x_1,x_2,x_3,x_4)x_2{}^{-\alpha[(p_2-k)^2]-1}$$
$$\times x_4{}^{-\alpha[(p_4-k)^2]-1}. \quad (3.2)$$

The region $x_2\sim0$, $x_4\sim0$ in the integration in Eq. (3.2) gives rise to zero-spin poles in $I(k)$ at $\alpha[(p_2-k)^2]=\alpha[(p_4-k)^2]=0$. In the vicinity of these poles,

$$I(k)\sim\{\alpha[(p_2-k)^2]\alpha[(p_4-k)^2]\}^{-1}I^{00}(k), \quad (3.3)$$

where

$$I^{00}(k)=\int dx_1dx_3I(k;x_1,0,x_3,0). \quad (3.4)$$

From Eq. (2.2) we have

$$I^{00}(k)=\int dx_1dx_3x_1{}^{-\alpha(t_1)-1}(1-x_1)^{-\alpha(u_1)-1}$$
$$\times x_3{}^{-\alpha(t_2)-1}(1-x_3)^{-\alpha(u_2)-1}R(x_1,0,x_3,0), \quad (3.5)$$

where

$$t_1=(p_1-k)^2,\quad t_2=(p_3-k)^2,\quad s+t_i+u_i=4m^2\quad(i=1,2).$$

In order that $I^{00}(k)$ represent the product of two Veneziano four-point functions (2.1), we must have

$$R(x_1,0,x_3,0)=f(x_1)f(x_3), \quad (3.6)$$

from which it follows that

$$I^{00}(k)=V(u_1,t_1)V(u_2,t_2). \quad (3.7)$$

The zero-spin mass-shell contribution to $I^{(a)}(s,t)$ is thus

$$I_{\rm cut}{}^{(a)00}(s,t)=(i\pi)^2\int d^4k\,\theta(p_2{}^0-k^0)$$
$$\times\delta(\alpha[(p_2-k)^2])\theta(p_4{}^0-k^0)$$
$$\times\delta(\alpha[(p_4-k)^2])V(u_1,t_1)V(u_2,t_2). \quad (3.8)$$

We can express the integral (3.8) for asymptotic s in terms of an integration over the initial and final momentum transfers t_1 and t_2 as

$$I_{\rm cut}{}^{(a)00}(s,t)=-\frac{\pi^2}{4q\sqrt{s}}$$
$$\times\int\frac{dt_1dt_2}{(-K)^{1/2}}\theta((-K)^{1/2})V(u_1,t_1)V(u_2,t_2), \quad (3.9)$$

where q is the c.m. momentum and

$$K=t^2+t_1{}^2+t_2{}^2-2t_1t_2-2tt_1-2tt_2.$$

We can compute $I_{\rm cut}{}^{(a)00}(s,t)$ asymptotically by replacing the V by their asymptotic forms

$$V(u_i,t_i)\sim\Gamma(-\alpha(t_i))s^{\alpha(t_i)}f(0)\quad\text{as } s\to\infty. \quad (3.10)$$

Then, asymptotically,

$$I_{\rm cut}{}^{(a)00}(s,t)=\int_{-\infty}^{\alpha_c(t)}dj\,s^j\rho_{\rm cut}{}^{00}(j,t), \quad (3.11)$$

where

$$\rho_{\rm cut}{}^{00}(j,t)=-\tfrac{1}{2}\pi^2f^2(0)$$
$$\times\int\frac{dt_1dt_2}{(-K)^{1/2}}\theta((-K)^{1/2})\delta(j+1-\alpha(t_1)-\alpha(t_2))$$
$$\times\Gamma(-\alpha(t_1))\Gamma(-\alpha(t_2)). \quad (3.12)$$

Asymptotically, we have [as in Eq. (2.15)]

$$I_{\rm cut}{}^{(a)00}(s,t)\sim(s^{\alpha_c(t)}/\ln s)\rho_{\rm cut}{}^{00}(\alpha_c(t),t)[1+O(1/\ln s)]. \tag{3.13}$$

If we take $\alpha(s)=\alpha(0)+s$, we can evaluate $\rho_{\rm cut}{}^{00}(\alpha_c(t),t)$ directly from Eq. (3.12) as

$$\rho_{\rm cut}{}^{00}(\alpha_c(t),t)=-\tfrac{1}{2}\pi^2 f^2(0)\times\int dt_1dt_2\pi\delta(t_1-t_2)\delta(\tfrac{1}{2}t-t_1-t_2)\times\Gamma(-\alpha(t_1))\Gamma(-\alpha(t_2))$$
$$=-\tfrac{1}{4}\pi^3 f^2(0)\Gamma^2(-\alpha(\tfrac{1}{4}t)). \tag{3.14}$$

Comparing Eqs. (2.16) and (3.14) we see that, although the cut spectral functions $\rho_{\rm cut}{}^{00}(j,t)$ and $\rho_{\rm cut}(j,t)$ are not simply related for arbitrary j, they are simply related (and have the same singularity structure) at the endpoint $j=\alpha_c(t)$, the point that gives the leading asymptotic behavior.

At $j=\alpha_c(t)$ we have [from Eqs. (2.16) and (3.14)]

$$\rho_{\rm cut}(\alpha_c(t),t)=\Lambda(t)\rho_{\rm cut}{}^{00}(\alpha_c(t),t), \tag{3.15}$$

where $\Lambda(t)$ is the slowly varying exponential (for small t)

$$\Lambda(t)=[2f(\tfrac{1}{2})/f(0)]^2 2^{-t}. \tag{3.16}$$

The factor 2^{-t} arises because the moving cut in the nonplanar Feynman-like diagram, Fig. 1, comes from the region of integration $(0,\frac{1}{2},0,\frac{1}{2})$, whereas the cut in the on-mass-shell double scattering comes from the region (0,0,0,0).

If $I_{\rm cut}{}^{(b)00}(s,t)$ is the Regge-cut amplitude due to putting the intermediate state in Fig. 1(b) on its zero-spin mass shell, we have [cf. Eq. (3.9)]

$$I_{\rm cut}{}^{(b)00}(s,t)=-\frac{\pi^2}{4q\sqrt{s}}\times\int\frac{dt_1dt_2}{(-K)^{1/2}}\theta((-K)^{1/2})V(s,t_1)V(s,t_2). \tag{3.17}$$

As $s\to\infty$ above the wedge containing the real axis,

$$V(s,t_i)\to e^{-i\pi\alpha(t_i)}s^{\alpha(t_i)}\Gamma(-\alpha(t_i))f(0). \tag{3.18}$$

Thus, for $s\to\infty$ above the wedge,

$$I_{\rm cut}{}^{(b)00}(s,t)=-\int_{-\infty}^{\alpha_c(t)}dj\,e^{-i\pi j}s^j\rho_{\rm cut}{}^{00}(j,t). \tag{3.19}$$

Note the minus sign in Eq. (3.19) compared to Eq. (2.17).

The heuristic double-scattering Regge cut[10,13] is given in terms of $I^{(a)}$ and $I^{(b)}$ as[14]

$$I_{\rm cut}{}^{00}(s,t)=-2i[I_{\rm cut}{}^{(a)00}+I_{\rm cut}{}^{(b)00}]. \tag{3.20}$$

[13] If A^{ik} and A^{kj} are the partial-wave amplitudes for the scattering processes $i\to k$, $k\to j$, the double-scattering cut amplitude is given by $I_{\rm cut}{}^{ij}=\frac{1}{2}iA^{ij}A^{jk}$ (see Ref. 10).

[14] The additional factor of -4 arises because $I^{(a)}$ and $I^{(b)}$ differ from the A's in Ref. 13 by a factor $2i$.

Thus

$$I_{\rm cut}{}^{00}(s,t)=-2i\int_{-\infty}^{\alpha_c(t)}dj[1-e^{-i\pi j}]s^j\rho_{\rm cut}{}^{00}(j,t) \tag{3.21}$$
$$=2\int_{-\infty}^{\alpha_c(t)}dj[1+e^{i\pi j}]\times\tan(\tfrac{1}{2}\pi j)s^j\rho_{\rm cut}{}^{00}(j,t), \tag{3.22}$$

showing that the combination of Figs. 1(a) and 1(b) gives a double-scattering cut with the correct signature.

Although $\rho_{\rm cut}(j,t)$ and $\rho_{\rm cut}{}^{00}(j,t)$ are similar at $j=\alpha_c(t)$, the effect of the extra term $\tan(\frac{1}{2}\pi j)$ in Eq. (3.22) is to alter the positions of the zeros in the asymptotically leading term in the double-scattering cut amplitude (in comparison to the Feynman-like cut amplitude).

Thus asymptotically we have

$$I_{\rm cut}{}^{00}(s,t)\sim 2(s^{\alpha_c(t)}/\ln s)(1+e^{-i\pi\alpha_c(t)})\times\tan(\tfrac{1}{2}\pi\alpha_c(t))\rho_{\rm cut}{}^{00}(\alpha_c(t),t)[1+O(1/\ln s)]. \tag{3.23}$$

Comparing Eq. (3.23) with Eq. (2.19) with the aid of Eq. (3.15), we see that $I_{\rm cut}(s,t)$ and $I_{\rm cut}{}^{00}(s,t)$ have the same singularity structure, but $I_{\rm cut}(s,t)$ has zeros in the leading term (which will be partially filled by nonvanishing lower-order terms) at $\alpha_c(t)=-2n$ (n integer), whereas $I_{\rm cut}{}^{00}(s,t)$ has zeros in its leading term at $\alpha_c(t)=-2n-1$ (n integer).[15]

We conclude this section by briefly discussing higher-spin mass-shell Regge-cut amplitudes, since higher-spin (than that of the initial- and final-state particles) on-mass-shell intermediate states are not excluded in the multiple-scattering formalism.[3,10] Unfortunately, there is no reliable way to determine which states should be included without double counting,[16] and their inclusion is usually simulated by introducing scale factors as essentially arbitrary parameters.[3]

Let $I_{\rm cut}{}^{(a)mn}(s,t)$ be the Regge-cut amplitude obtained from Fig. 1(a) by putting the two-particle intermediate state on the mass shell, $\alpha[(p_2-k)^2]=m$, $\alpha[(p_4-k)^2]=n$. Then from Eqs. (3.1) and (3.2),

$$I_{\rm cut}{}^{(a)mn}(s,t)=\frac{(i\pi)^2}{m!n!}\int d^4k\;\theta(p_2{}^0-k^0)\delta(\alpha[(p_2-k)^2]-m)\times\theta(p_4{}^0-k^0)\delta(\alpha[(p_4-k)^2]-n)\times\int dx_1dx_3\frac{\partial^{m+n}}{\partial x_2{}^m\partial x_4{}^n}I(k,x_1,x_2,x_3,x_4)\Big|_{x_2=x_4=0}. \tag{3.24}$$

[15] This is to be compared with the two-particle unitarity cut from Figs. 1(a) and 1(b) which gives the asymptotic amplitude

$$I_{\rm cut}{}^{\rm unit00}(s,t)\sim-(2s^{\alpha_c(t)}/\ln s)(1+e^{-i\pi\alpha_c(t)})/\csc\pi\alpha_c(t)\rho_{\rm cut}{}^{00}(\alpha_c(t),t).$$

We see that the factor $\csc\pi\alpha_c(t)$ introduces poles in $I_{\rm cut}$ at $\alpha_c(t)=-2n$ (n integer), which makes comparison difficult.

[16] See P. G. O. Freund [Phys. Rev. Letters **22**, 565 (1969)] for one prescription for on-mass-shell intermediate-state counting.

To compute the right-hand side of Eq. (3.24), we need knowledge of the spectral function $R(x_1x_2x_3x_4)$. In general, $I_{\text{cut}}{}^{(a)mn}(s,t)$ will be of the form (asymptotically in s)

$$I_{\text{cut}}{}^{(a)mn}(s,t) = -\tfrac{1}{2}\pi^2\int\frac{dt_1dt_2}{(-K)^{1/2}}\theta((-K)^{1/2})P^{m,n}(t_1,t_2)s^{\alpha(t_1)+\alpha(t_2)-1} \times f^2(0)\Gamma(-\alpha(t_1))\Gamma(-\alpha(t_2)), \quad (3.25)$$

where $P^{m,n}(t_1,t_2)$ is a polynomial of order $m+n$ in t_1 and t_2. To order $\ln^{-1}s$ we see that

$$I_{\text{cut}}{}^{(a)mn}(s,t)\sim -\tfrac{1}{4}\pi^3\Gamma^2(-\alpha(\tfrac{1}{4}t))P^{m,n}(\tfrac{1}{4}t,\tfrac{1}{4}t)f^2(0) = P^{m,n}(\tfrac{1}{4}t,\tfrac{1}{4}t)I_{\text{cut}}{}^{(a)00}(s,t). \quad (3.26)$$

Suppose $I_{\text{cut}}{}^{(a)\text{total}}(s,t)$ is the Regge-cut amplitude obtained from Fig. 1 by on-mass-shell double-scattering in which the intermediate states range over a set of values $\{m,n\}$ {for which $\alpha[(p_2-k)^2]=m$, $\alpha[(p_4-k)^2]=n$}. Then if (for asymptotic s) we can use the asymptotic form Eq. (3.26) for each intermediate state, we have

$$I_{\text{cut}}{}^{(a)\text{total}}(s,t)\sim\lambda(t)I_{\text{cut}}{}^{(a)00}(s,t), \quad (3.27)$$

where the scale factor[3]

$$\lambda(t)=\sum_{\{m,n\}}(I_{\text{cut}}{}^{(a)mn}/I_{\text{cut}}{}^{(a)00})$$

is a polynomial in t of degree $M+N$, where $M=\max m$, $N=\max n$.

It might be possible, for example, to choose $\{m,n\}$ so that $\rho_{\text{cut}}{}^{(a)\text{total}}(\alpha_c(t),t)\approx\rho_{\text{cut}}(\alpha_c(t),t)$ [Eq. (2.16)] for small t, since $\Lambda(t)$ [Eq. (3.16)] is a rapidly converging power series. However, the different method of constructing the signature factor in Feynman-like and on-shell scattering methods will still give an extra factor of $\tan(\frac{1}{2}\pi\alpha_c(t))$ in the latter, displacing the positions of the zeros.

4. CONCLUSION

We have computed the Regge-cut amplitudes obtained from Fig. 1(a) using two methods: (i) by considering it as a Feynman-like diagram and (ii) by putting the intermediate two-particle state on the zero-spin mass shell of the external particles.

Both Regge cuts have the same branch point $j=\alpha_c(t)$, and although the cut spectral functions $\rho(j,t)$ are not simply related for arbitrary j, they are simply related (with the same singularities outside the s-channel physical region) at the branch-point $j=\alpha_c(t)$, at which point their ratio is a slowly varying exponential in t. It is possible that the inclusion of higher-spin mass-shell intermediate states in method (ii) could make the similarity still greater for small t.

Since the asymptotic cut amplitudes are given by $\rho(\alpha_c(t),t)$, the similarity between the spectral functions leads to asymptotic similarity between the Regge-cut amplitudes obtained from Fig. 1(a) by methods (i) and (ii).

The main difference between the two methods arises in the way the $s\leftrightarrow u$ crossing diagram Fig. 1(b) is included. Treated as a Feynman-like diagram, the combination of Fig. 1(a) and Fig. 1(b) gives the signature factor $(1+e^{-i\pi j})$ directly. However in the mass-shell double-scattering formalism, the signature factor is introduced as $-i(1-e^{-i\pi j})=(1+e^{-i\pi j})\tan(\frac{1}{2}\pi j)$. The two methods thus give rise to zeros in the asymptotic cut amplitudes at different values of t.

This suggests that, although the on-mass-shell double-scattering Regge cut could reproduce the qualitative features of the two-Reggeon cut (obtained from the Feynman-like Fig. 1 by the methods of Ref. 7), the detailed quantitative predictions of such a cut would be incorrect.

In conclusion we note[6] that the amplitude $I(s,t)$ [Eq. (2.2)] will not give complete factorizability of lower daughters. Requiring complete factorizability would give rise to an additional singularity because of the great degeneracy of lower daughters. Nonetheless, we expect the general conclusions of this paper to be valid in a more complete theory.

APPENDIX: RELATIONSHIP BETWEEN DEPENDENT VARIABLES IN DUAL DIAGRAM

In this appendix we reproduce from Kikkawa *et al.*[6] the expression relating two variables connected by duality (corresponding to intersecting lines in the dual diagram). Let x and y be the diagonals of a quadrilateral in the dual diagram with sides a_1, a_2, a_3, and a_4 (Fig. 3). Then

$$y=f(x:a_1,a_2,a_3,a_4), \quad (A1)$$

where f satisfies

$$f(x:a_1,a_2,a_3,a_4)=f(x:a_4,a_3,a_2,a_1) =f(x:a_2,a_1,a_4,a_3) \quad (A2)$$

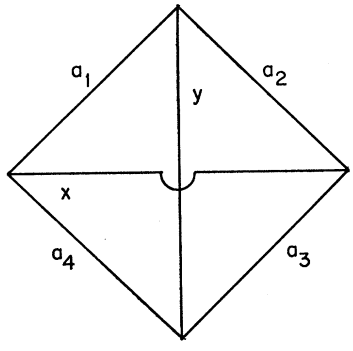

FIG. 3. Part of a dual diagram.

and

$$y=f(x:a_1,a_2,a_3,a_4)\Rightarrow x=f(y:a_1,a_4,a_3,a_2). \quad \text{(A3)}$$

The function f can be written implicitly as

$$f(x:a_1,a_2,a_3,a_4)=\frac{1-x\alpha_2\alpha_3}{1-x\alpha_2\alpha_3a_1}\,\frac{1-x\alpha_2\alpha_3a_1a_4}{1-x\alpha_2\alpha_3a_4}, \quad \text{(A4)}$$

where

$$a_2=\frac{1-\alpha_2}{1-\alpha_2a_1}\,\frac{1-\alpha_2a_1x}{1-\alpha_2x}$$

and

$$a_3=\frac{1-\alpha_3}{1-\alpha_3a_4}\,\frac{1-\alpha_3a_4x}{1-\alpha_3x}. \quad \text{(A5)}$$

PHYSICAL REVIEW VOLUME 188, NUMBER 5 25 DECEMBER 1969

Regge-Pole Model of Elastic Large-Angle Scattering at High Energies*

NAOHIKO MASUDA
Department of Physics, University of Wisconsin, Madison, Wisconsin 53706
and
Department of Physics, Louisiana State University, Baton Rouge, Louisiana 70803†

AND

SHOJI MIKAMO‡
Physical Sciences Laboratory, University of Wisconsin, Stoughton, Wisconsin 53589

(Received 17 October 1968)

The effect of the Regge-pole-like structure of an amplitude in the small-angle region on the behavior of the high-energy elastic large-angle scattering is studied by linearizing the nonlinear integral equation for the imaginary part of the amplitude derived from the unitarity relation. It is shown that the slope of the elastic large-angle differential cross section for antiparticle-particle scattering should be always less steep than that of large-angle particle-particle scattering, contrary to the situation in the small-angle region. Using the general formula for the elastic large-angle scattering obtained in this paper, we analyze numerically the existing experimental data on the $\bar{p}p$ and pp differential cross sections at large angles. With regard to the logarithmic slopes of the differential cross sections, we found that this model can reproduce the gross structure of the experimental data on both $\bar{p}p$ and pp processes. Our prediction that the slope of the $\bar{p}p$ large-angle scattering cross section will be less steep than that of pp is also confirmed experimentally. The dip and bump structures in experimental differential cross sections are compared with the theoretical prediction of oscillations in the differential cross section.

I. INTRODUCTION

BOTH experimental and theoretical studies of large-angle elastic scattering at high energies have recently attracted much attention.

Considerable amounts of experimental data on large-angle elastic differential cross sections for various processes are available.[1,2] A common feature of large-angle elastic scattering is the strong decrease of the differential cross section with increasing angle, although the slope is less steep than that in the small-angle region Orear[3] proposed the following empirical formula to describe the general behavior of the elastic differential cross section at large angles:

$$d\sigma/d\Omega=A\,\exp(-bp\,\sin\theta), \quad (1)$$

where A and b are positive constants, and p and θ are the c.m. three-momentum and scattering angle, respectively.

Recent precise experiments[1] have, however, revealed that, although Orear's empirical formula (1) reproduces the gross features of the experimental differential cross sections, there exist substantial deviations from Eq. (1) which may be interpreted as dip structures or oscillations.

Since the proposal of Orear's empirical formula (1), several theoretical models of large-angle elastic scattering which lead to differential cross sections similar to Eq. (1) have been studied. One of the most attractive

* Work supported in part by the University of Wisconsin Research Committee, with funds granted by the Wisconsin Alumni Research Foundation, in part by the U. S. Atomic Energy Commission, under Contract No. At(11-1)-881, COO-197 and in part by NSF Grant No. GJ-132 to the LSU Computer Research Center.

† Present address.

‡ Present address: Institute for Nuclear Study, University of Tokyo, Tanashi-shi, Tokyo, Japan.

[1] Review article for experimental data on elastic large angle pp scattering: T. V. Allaby *et al.*, in *Proceedings of the Topical Conference on High-Energy Collisions of Hadrons* (CERN, Geneva, 1968); CERN Report No. 68-7, p. 580 (unpublished).

[2] Review article for some earlier experimental data on elastic large angle $\bar{p}p$ scattering: M. L. Perl, in *Proceedings of the Topical Conference on High-Energy Collisions of Hadrons* (CERN, Geneva, 1968); CERN Report No. 68-7, p. 252 (unpublished).

[3] J. Orear, Phys. Rev. Letters **12**, 112 (1964).